THE JOURNAL OF IMMUNOLOGY

Nanoparticle-Mediated Combinatorial Targeting of Multiple Human Dendritic Cell (DC) Subsets Leads to Enhanced T Cell Activation via IL-15–Dependent DC Crosstalk

Kartik Sehgal, Ragy Ragheb, Tarek M. Fahmy, Madhav V. Dhodapkar and Kavita M. Dhodapkar

J Immunol published online 30 July 2014
http://www.jimmunol.org/content/early/2014/07/30/jimmunol.1400489

The Journal of Immunology is published twice each month by The American Association of Immunologists, Inc., 9650 Rockville Pike, Bethesda, MD 20814-3994.

Print ISSN: 0022-1767 Online ISSN: 1550-6606.

Published July 30, 2014, doi:10.4049/jimmunol.1400489

Nanoparticle-Mediated Combinatorial Targeting of Multiple Human Dendritic Cell (DC) Subsets Leads to Enhanced T Cell Activation via IL-15–Dependent DC Crosstalk

Kartik Sehgal,*,† Ragy Ragheb,‡ Tarek M. Fahmy,‡,§ Madhav V. Dhodapkar,†,§,¶ and Kavita M. Dhodapkar*,¶

Most vaccines depend on coadministration of Ags and adjuvants that activate APCs. Nanoparticles (NPs) have emerged as an attractive vehicle for synchronized delivery of Ags and adjuvants to APCs and can be targeted to specific cell types, such as dendritic cells (DCs), which are potent APCs. Which subset of human DCs should be targeted for optimal activation of T cell immunity, however, remains unknown. In this article, we describe a poly-lactic-coglycolic acid–based NP platform, wherein avidin-decorated NPs can be targeted to multiple human DC subsets via biotinylated Abs. Both BDCA3$^+$ and monocyte-derived DC-SIGN$^+$ NP-loaded DCs were equally effective at generating Ag-specific human T cells in culture, including against complex peptide mixtures from viral and tumor Ags across multiple MHC molecules. Ab-mediated targeting of NPs to distinct DC subsets led to enhanced T cell immunity. However, combination targeting to both DC-SIGN and BDCA3$^+$ DCs led to significantly greater activation of T cells compared with targeting either DC subset alone. Enhanced T cell activation following combination targeting depended on DC-mediated cytokine release and was IL-15 dependent. These data demonstrate that simultaneous targeting of multiple DC subsets may improve NP vaccines by engaging DC crosstalk and provides a novel approach to improving vaccines against pathogens and tumors. ***The Journal of Immunology*****, 2014, 193: 000–000.**

Dendritic cells (DCs) play a central role in regulating innate and adaptive immunity and hence there is great interest in targeting these cells to improve the effectiveness of vaccines against both pathogens as well as cancer. The existence of different DC subsets with distinct functions, as well as the ability of DCs to undergo phenotypic and functional changes in response to external stimuli, allows them to regulate diverse types of immune responses (1, 2). Most of the adjuvants in current vaccines are thought to act in part via activating DCs. Owing in part to their potency, several investigators have tried to target Ags to DCs in vivo to boost immunity and improve vaccines (3, 4). One approach involves protein Ags coupled to DC-targeting Abs (such as DEC-205), which is currently in clinical trials (5). Another strategy involves coupling DC-targeting strategy to other Ag delivery vehicles (6).

Synchronized delivery of Ag and adjuvants to APCs is thought to be critical for vaccine design. In addition to chemical cross-linking, several vehicles such as poly-lactic-coglycolic acid (PLGA) polymeric nanoparticles (NPs), liposomes, nanocrystals, virus-like particles, and 3D-scaffolds have been explored as vehicles for delivering Ags and adjuvants to APCs (7–10). Polymeric NPs fabricated from Food and Drug Administration–approved polymers such as PLGA are an attractive platform for vaccines owing to their established safety in human studies, lack of off-target effects, and ease of production (6, 8, 11, 12). Several studies have explored targeting of NPs to human or murine DCs or DC subsets via Abs against receptors expressed on DCs/subsets such as DC-SIGN, DEC-205, CLEC9A, DCIR, BDCA-2, and CD32 (13–18) or more generally against pathogen-associated molecular patterns (19). The rationale for targeting different DC subsets derives in part from differences in their functional properties. For example, in mice, the CD8α^+ subset of DCs is specialized at cross-presentation of exogenous Ags to generate cytolytic T cells (20, 21). BDCA3$^+$ myeloid DCs (MDCs) were identified as human counterparts of CD8α^+ DCs and potentially attractive targets for DC-targeting vaccines (22). However, recent studies suggest that several subsets of lymph node resident human DCs may be equally efficient at cross-presentation of soluble Ag (23). Cross-presentation of Ab-targeted Ag by human BDCA3$^+$ MDCs was instead shown to depend on the nature of the endocytic compartment targeted (24). Therefore, at least some aspects of the biology of murine DC subsets may not translate readily to human DCs, and the nature of optimal DC subsets for NP-mediated targeting in humans remains to be determined (25). In this study, we have used a novel PLGA-NP platform wherein the particles are decorated with avidin (26, 27) and loaded with clinically relevant viral and tumor Ags, allowing facile exploration of Ab-mediated targeting of different DC subsets via NPs. These data demonstrate, for the first time to our knowledge, the potential advantages of NP vaccines for multivalent Ag delivery and simultaneous targeting of several DC subsets.

*Department of Pediatrics, Yale School of Medicine, Yale University, New Haven, CT 06510; †Department of Medicine, Yale School of Medicine, Yale University, New Haven, CT 06510; ‡Department of Biomedical Engineering, Yale School of Engineering, Yale University, New Haven, CT 06510; §Department of Immunobiology, Yale School of Medicine, Yale University, New Haven, CT 06510; and ¶Yale Cancer Center, Yale School of Medicine, Yale University, New Haven, CT 06510

Received for publication February 20, 2014. Accepted for publication June 30, 2014.

This work was supported by National Institutes of Health Grant R01AI079222, a grant from The Dana Foundation (to K.M.D.), National Institutes of Health Grants CA106802 and CA135110, the Multiple Myeloma Research Foundation, the Bunker Professorship (to M.V.D.), and National Institutes of Health Grant R01AR064350 and Pilot Grant U19AI082713 (to T.M.F.).

Address correspondence and reprint requests to Dr. Kavita M. Dhodapkar, Pediatric Hematology and Oncology Program, Yale Cancer Center, Yale School of Medicine, Yale University, 333 Cedar Street, New Haven, CT 06510. E-mail address: kavita.dhodapkar@yale.edu

The online version of this article contains supplemental material.

Abbreviations used in this article: DC, dendritic cell; FMP, influenza-matrix peptide; MDC, myeloid DC; MFI, mean fluorescence intensity; Mo-DC, monocyte-derived DC; NP, nanoparticle; PLGA, poly-lactic-coglycolic acid; poly(I:C), polyinosinic–polycytidylic acid.

Materials and Methods

Generation of peptide-loaded NPs

PLGA NPs containing avidin on the surface were prepared (see Fig. 1A–C or characterization of NPs and Supplemental Table I for NP composition), using methods described earlier (27, 28). The NPs prepared included blank NP (no peptide), coumarin-labeled blank NP (NP-coumarin), NP–influenza-matrix peptide (FMP) (incorporating HLA A2.1 FMP sequence GILGFVFTL), NP-CEF (incorporating CEF pool peptide, pool of 32 peptides from EBV, CMV, and influenza virus, Anaspec), and NP-SOX2 (22 15-mer SOX2 peptides; Supplemental Table II). The amount of each peptide in the NPs was as follows: NP-FMP (9 μg/mg NP); NP-CEF (0.56 μg/mg NP), and NP-SOX2 (4.1 μg/mg NP) (Supplemental Table I). In some experiments, TLR and/or Ab-coated NPs were prepared by adding biotinylated LPS (InvivoGen), polyinosinic–polycytidylic acid [poly (I:C)] (InvivoGen), BDCA3 Ab (Miltenyi Biotec), or DC-SIGN Ab (Miltenyi Biotec) at the concentration of 5 μg Ab per milligram of NPs. The vials were gently rotated for 15 min. They were then centrifuged at 1200 rpm for 5 min to remove the supernatant and washed twice to remove any soluble ligand prior to use in experiments.

NP uptake experiments

NPs loaded with coumarin as a marker were added to PBMCs for 30 min at varying concentrations (5.5, 55, and 110 μg/ml) at either 37˚C or 4˚C. Flow cytometry was performed and mean fluorescence intensity (MFI)–coumarin analyzed to evaluate the uptake of NPs by monocytes, MDCs, B cells, NK cells, and T cells, using anti-human CD14, BDCA3, CD19, CD56, and CD3 Abs, respectively.

Generation of DCs

Monocyte-derived DCs (Mo-DCs) were generated from PBMCs, as described (29). Briefly, $CD14^+$ monocytes were isolated from PBMCs by immunomagnetic bead selection using CD14 beads following the manufacturer's protocol (Miltenyi Biotec). $CD14^+$ cells were suspended in 1% healthy donor plasma in RPMI 1640 (Cellgro), supplemented with IL-4 (25 μg/ml; R&D Systems) and GM-CSF (20 ng/ml sargramostim [Leukine]; Genzyme) on days 0, 2, and 4 of culture. Immature Mo-DCs were harvested on days 5-6 and used for the experiments described below. The $CD14^-$ fraction of PBMCs was cultured in the presence of 5% pooled human serum (Labquip) in RPMI 1640. For some experiments, $BDCA3^+$ MDCs were isolated from the PBMCs using BDCA3 MACS beads (Miltenyi Biotec).

Ag-specific T cell stimulation

Day 6 immature Mo-DCs or freshly isolated $BDCA3^+$ MDCs were loaded with either blank NPs or NPs encapsulated with FMP, NP-FMP (1 h); CEF pool peptide, NP-CEF (1 h); or SOX2 pool peptide, NP-SOX2 (4 h). After overnight culture in 1% plasma, NP-loaded DCs were used to stimulate autologous T cells at a DC/T cell ratio of 1:30 in the presence of IL-2 (10 μg/ml at days 4 and 7; Chiron). After 10–12 d in culture, flow cytometry was performed to detect the presence of Ag-specific T cells, using A2.1 FMP tetramer (Beckman Coulter), as well as intracellular cytokine secretion assay for IFN-γ, with the peptides used for initial T cell stimulation in the presence of anti-CD28 and anti-CD49D (1 μg/ml).

For experiments with NP-SOX2, T cells were restimulated with NP-loaded DCs on days 7 and 14 in the presence of IL-2 (10 μg/ml) as well as IL-7 and IL-15 (both at 5 μg/ml; R&D Systems). For some experiments, DCs were matured overnight with LPS (50 ng/ml; Sigma-Aldrich) or poly(I:C) (25 μg/ml; Sigma-Aldrich) or cytokine mixture [IL-6 (0.01 μg/ml; R&D Systems), IL-1β (0.01 μg/ml; R&D Systems), TNF-α (0.01 μg/ml; R&D Systems), and PGE_2 (1 μg/ml, Sigma-Aldrich)] after loading with NPs.

For targeting experiments, BDCA3 or DC-SIGN Ab–coated NPs were added to PBMCs at 4˚C for 1 h, washed, and cultured for 10–14 d in the presence of IL-2 (10 μg/ml on days 4 and 7). In some experiments, these were compared with a combinatorial targeting approach in which both BDCA3 and DC-SIGN–coated NPs were added at half concentrations. In additional experiments, neutralizing Abs against cytokines IL-15, IFN-λ, IL-6, or isotype control mouse IgG1 (all 10 μg/ml; R&D Systems) were added to the combinatorial targeting condition. Flow cytometry was performed for the detection of Ag-specific T cells, as described above. The flow cytometry data were acquired using CellQuest (BD) software on FACSCalibur. The data were then analyzed using FlowJo software (TreeStar).

Cytokines produced by $BDCA3^+$ MDCs

$BDCA3^+$ MDCs isolated from healthy donor buffy coats or $DC\text{-}SIGN^+$ Mo-DC were loaded with NP-FMP at 37˚C and supernatants were collected after 24 h. Cytokines were quantified using VeriPlex Human Cytokine ELISA (PBL IFN source) and data were analyzed by Q-View 2.160 software (Quansys Biosciences).

Statistical analysis

Two-tailed paired or ratio paired *t* tests were used to investigate the significance among the results. A p value < 0.05 was considered significant.

Results

Uptake and presentation of Ag-loaded NPs by human DCs/subsets

We first examined the relative uptake of NPs by different cellular components of human PBMCs (characteristics of the NPs are shown in Fig. 1). Coumarin-labeled NPs cultured with PBMCs were preferentially taken up by APCs, including $BDCA3^+$ MDCs as well as $CD14^+$ monocytes, as compared with B cells, NK cells, and T cells, in a concentration-dependent fashion (Fig. 2A, 2B). Uptake of NPs by DCs was an active process and inhibited by incubation at 4˚C (Fig. 2C). Next, we compared the capacity of Mo-DCs and $BDCA3^+$ MDCs to stimulate FMP-specific T cells

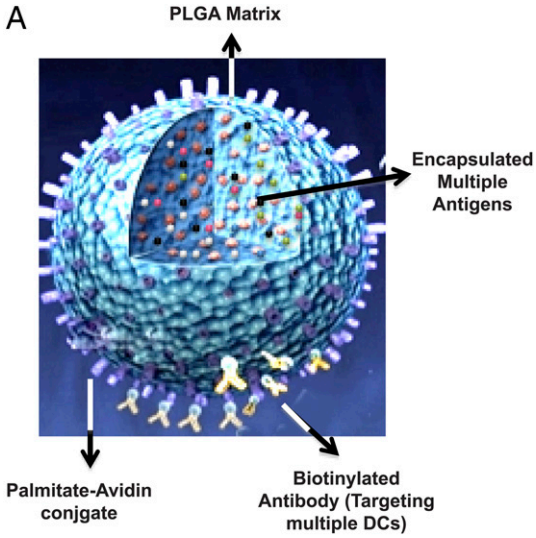

B

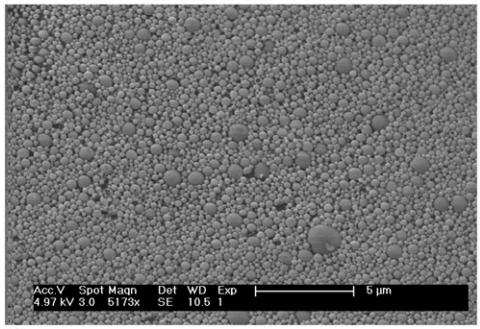

C

Surface Modification of Particle	Average Diameter	Poly dispersity
None	180±4 nm	0.20
Antibody-NP	210±7nm	0.25

FIGURE 1. Structure and characterization of NPs. (**A**) Structure of the NPs. NPs consist of PLGA matrix encapsulating Ags of interest. The surface of the NPs is decorated with palmitate avidin conjugate, which allows easy conjugation of targeting Abs coupled to biotin. (**B**) Characterization of NPs using the scanning electron microscope. (**C**) NPs were sized using dynamic light scattering (Malvern Zetasize).

following uptake of NP-FMP. Both Mo-DCs and BDCA3$^+$ MDCs were equally efficient at inducing proliferation of FMP-tetramer$^+$ T cells with the ability to secrete IFN-γ in response to peptide stimulation (Fig. 2D, 2E).

Vaccines with a single peptide epitope are by definition restricted to a single HLA type. To examine if the current platform could be extended to complex peptide mixtures to induce reactivity against multiple epitopes, we developed PLGA NPs containing a pool of 32 peptides from CMV, EBV, and influenza (flu) viruses (NP-CEF) recognized by different HLA haplotypes. Both Mo-DCs and BDCA3$^+$ MDCs were able to stimulate Ag-specific IFN-γ–secreting T cells in response to NP-CEF (Fig. 3A–C). Importantly, the elicited immune response included reactivities against multiple peptides within the mix (Fig. 3D, Supplemental Table 3).

Next we analyzed if this platform could be used to generate T cells against a tumor-associated Ag. To this end, we loaded NPs

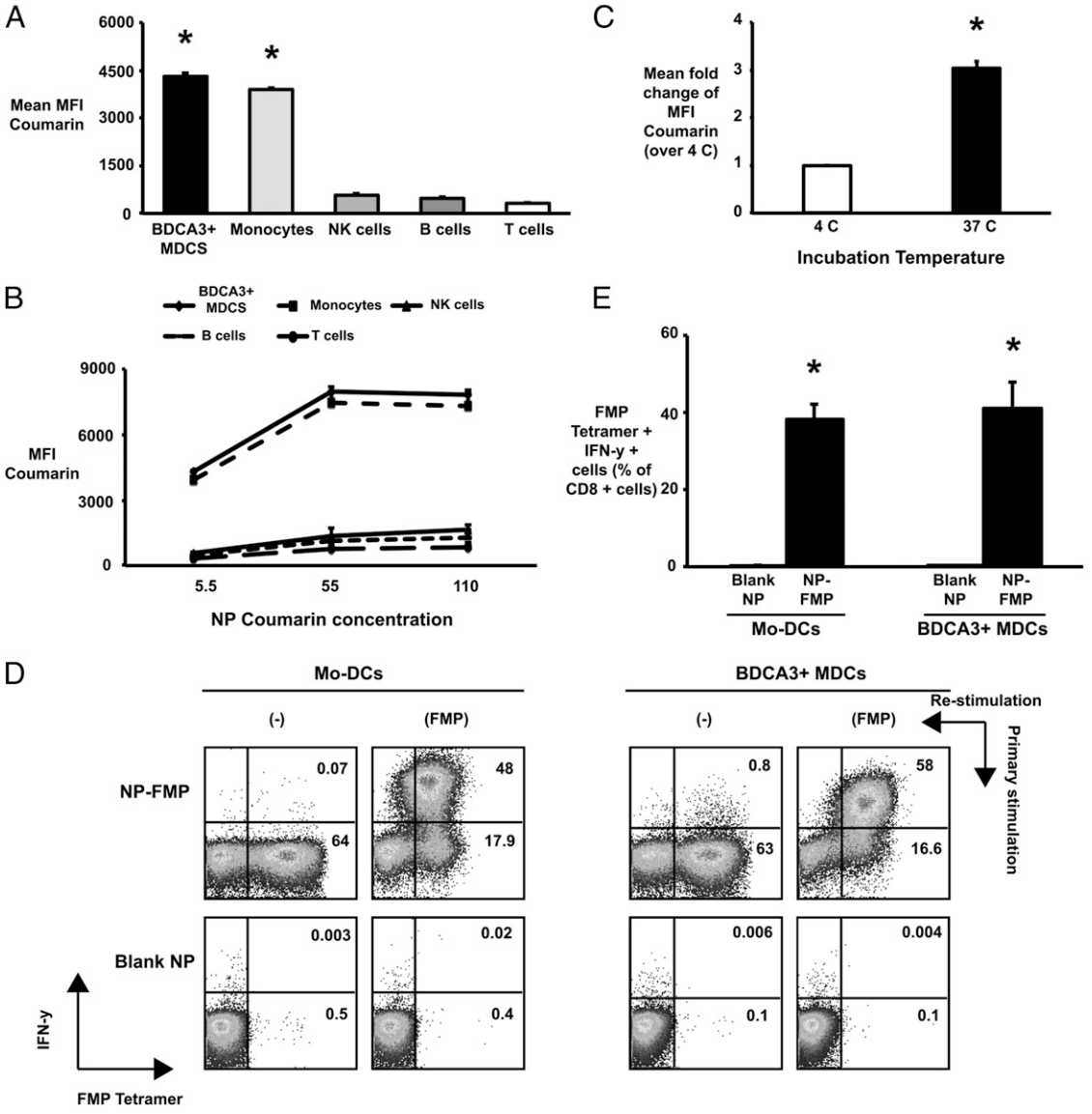

FIGURE 2. NPs are taken up by APCs preferentially, and peptide-loaded NPs lead to induction of Ag-specific T cell response. (**A**–**C**) Coumarin-labeled NPs (NP-coumarin) were used to study NP uptake by mononuclear cells using flow cytometry. MFI of coumarin was used to compare uptake by different cells. (A) PBMCs were incubated with NP-coumarin (5.5 μg/ml) for 30 min. NP uptake by BDCA3$^+$ MDCs, CD14$^+$ monocytes, CD19$^+$ B cells, CD3$^-$CD56$^+$ NK cells, and CD3$^+$ T cells was studied using flow cytometry to examine MFI of coumarin as an indicator of NP uptake. The bar graph shows mean coumarin MFI ± SEM from experiments with three healthy donors. *$p < 0.05$, BDCA3$^+$ DCs and monocytes compared with B cells, NK cells, and T cells. (B) NP uptake by BDCA3$^+$ DCs, monocytes, B cells, NK cells, and T cells at different NP concentrations ($n = 3$). (C) NP uptake by BDCA3$^+$ MDCs at different incubation temperatures is shown ($n = 3$). (**D** and **E**) NP-FMPs stimulate a specific CD8 T cell functional response. Mo-DCs or BDCA3$^+$ MDCs from HLA A2.1$^+$ healthy donors were loaded with NP-FMP at an FMP concentration of 5 μg/ml and then cocultured with autologous T cells. DCs loaded with blank NPs (Blank NP) were used as negative controls. After 10–12 d, the cells were restimulated with soluble FMP (5 μg /ml) in the presence of anti-CD28 and anti-CD49D and analyzed for production of IFN-γ by flow cytometry. Data shown in the figure are gated on CD3$^+$ CD8$^+$ T cells. (D) Representative figure from healthy donor showing expansion of FMP tetramer$^+$ IFN-γ–producing T cells by Mo-DCs loaded with either blank NP or NP-FMP (*left panel*) and representative figure from healthy donor showing expansion of FMP tetramer$^+$ IFN-γ–producing T cells by BDCA3$^+$ MDCs loaded with either blank NP or NP-FMP (*right panel*). (E) The graphs show mean percentage ± SEM of IFN-γ–producing FMP tetramer$^+$ CD8 cells from healthy donors stimulated with NP-FMP–loaded Mo-DC ($n = 8$, *$p = 1.8 \times 10^{-5}$, blank NP versus NP-FMP) and BDCA3$^+$ MDCs ($n = 4$, *$p = 8.7 \times 10^{-3}$, blank NP versus NP-FMP).

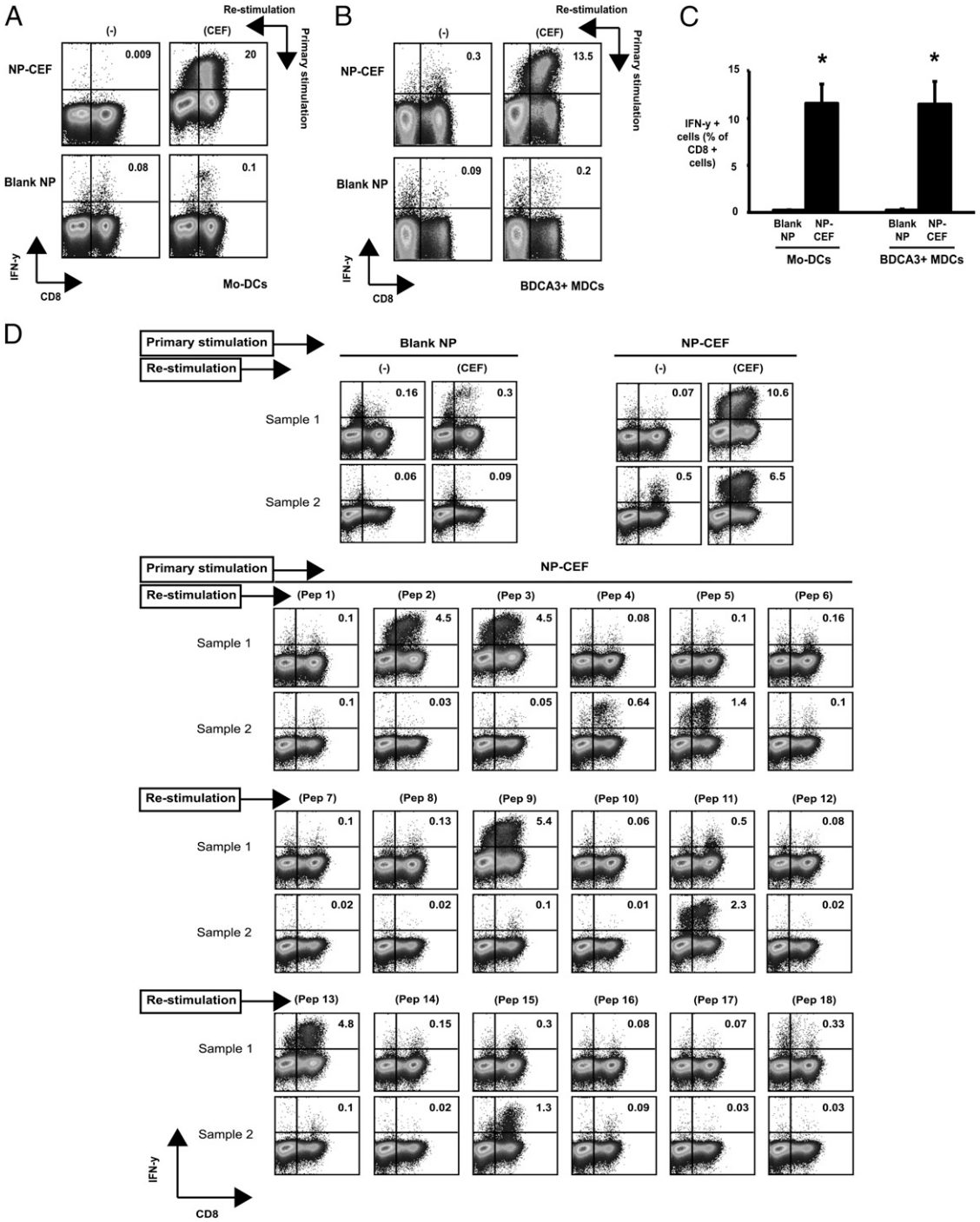

FIGURE 3. Complex peptide NPs encapsulating CEF pool peptide (NP-CEF) stimulate a specific and multivalent CD8 T cell functional response. Mo-DCs or BDCA3$^+$ MDCs were loaded with NP-CEF at an individual peptide concentration of 0.5 μg/ml and then cocultured with a CD14$^-$ fraction of PBMCs. DCs loaded with blank NPs (blank NP) were used as negative controls. After 10–12 d, the cells were restimulated with soluble CEF pool peptide (5 μg/ml) and analyzed for production of IFN-γ by flow cytometry. FACS plots shown in the figure are gated on CD3$^+$ cells. (**A**) Representative figure from healthy donor showing induction of Ag-specific IFN-γ producing CD8 lymphocytes in response to stimulation with either blank NP or NP-CEF–loaded autologous Mo-DCs. (**B**) Representative figure from healthy donor showing induction of Ag-specific IFN-γ–producing CD8 lymphocytes in response to stimulation with either blank NP or NP-CEF–loaded autologous BDCA3$^+$ MDCs. (**C**) The graph shows mean percentage (±SEM) of CD8 cells producing IFN-γ when stimulated by Mo-DCs ($n = 8$) or BDCA3$^+$ MDCs ($n = 3$) loaded with either blank NP or NP-CEF. *$p = 6 \times 10^{-4}$ (blank NP versus NP-CEF for Mo-DCs) and $p = 4.9 \times 10^{-2}$ (blank NP versus NP-CEF for BDCA3$^+$ MDCs). (**D**). The multivalent nature of response was confirmed by restimulating NP-CEF–stimulated cells with individual peptide components (Pep1–Pep18; described in Supplemental Table III) of CEF pool peptide. Representative examples with two different donors (Sample 1 and Sample 2) are shown. Blank NP and NP-CEF restimulated with CEF pool peptide were used as negative and positive controls, respectively.

with an overlapping peptide library derived from SOX2 (NP-SOX2). SOX2 has emerged as an important oncogene in several cancers, including lung cancer (30). In recent studies, we and others have implicated this Ag in protective immunity in the context of monoclonal gammopathy and in patients with lung cancer treated with anti-PD1 (programmed death) receptor Ab

(31, 32). We stimulated T cells using NP-SOX2–loaded autologous DCs. Because the peptides are 15 aa long, they require active processing for Ag presentation. DCs loaded with NP-SOX2 were able to stimulate both SOX2-specific CD4 and $CD8^+$ T cells in culture (Fig. 4). Taken together these data demonstrate that both $BDCA3^+$ and Mo-DC–$SIGN^+$ NP-loaded DCs are equally effective at generating Ag-specific human T cells in culture, including against complex peptide mixtures from viral and tumor Ags across multiple MHC molecules.

Targeting NPs to DC subsets

As noted earlier, the NPs are decorated with avidin on their surface, allowing facile coupling to biotinylated Abs for targeting. This coupling on the surface of NPs was confirmed by staining with a rat Ab against the C region of the biotinylated Ab (Supplemental Fig. 1A). Specificity of targeting to the $BDCA3^+$ and DC-$SIGN^+$ APCs was examined using flow cytometry to detect uptake of coumarin-labeled Ab–decorated NPs. Enhanced uptake of NPs was seen in the targeted APCs compared with nontargeted APCs (Supplemental Fig. 1B). Exposure of $BDCA3^+$ DCs and DC-$SIGN^+$ DCs to NPs leads to phenotypic maturation with upregulation of CD83, CD80, and CD86. Addition of poly(I:C)-coated NPs to $BDCA3^+$ DCs did not lead to further increase in expression of CD80, CD83, or CD86. Addition of LPS-coated particles to DC-SIGN DCs, however, led to further increase in CD86 (Supplemental Fig. 1C) when compared with noncoated NPs. For targeting experiments, peptide-loaded NPs were used at 100-fold lower concentrations to avoid nonspecific uptake of NPs by APCs. In contrast to prior studies wherein targeting of human DCs in culture was tested in the context of purified DCs, we examined the ability of Ab-targeted NPs to target DC subsets in the context of bulk mononuclear cells, wherein DC subsets, particularly $BDCA3^+$ MDCs, constitute only a minor fraction. Despite this, targeting of NPs to either the DC-$SIGN^+$ subset or $BDCA3^+$ MDCs led to enhanced activation of FMP-specific T cells (Fig. 5A, 5B). Both BDCA3- and DC-SIGN–targeted NPs led to similar increases in Ag-specific T cells over nontargeted NPs (Fig. 5C).

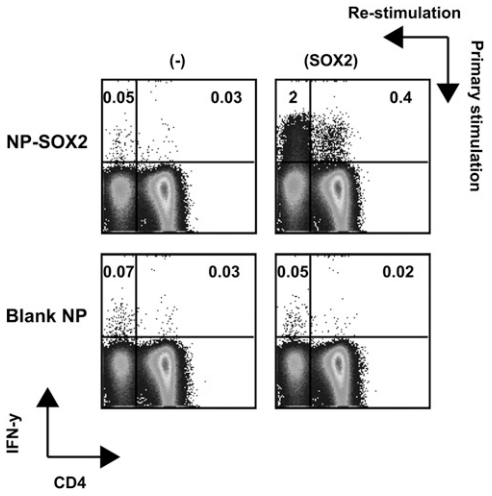

FIGURE 4. DCs targeted with NPs containing a complex mixture of long peptides from tumor Ag SOX2 lead to stimulation of Ag-specific CD4 as well as CD8 T cells. Day 5 immature Mo-DCs were cultured with SOX2 peptide containing NP (NP-SOX2, individual peptide concentration of 5 μg/ml), matured (using inflammatory cytokine mixture), and used to stimulate autologous T cells in the presence of IL-2 (10 μg/ml) and IL-7 and IL-15 (both at 10 ng/ml). The T cells were restimulated with NP-SOX2–loaded DCs on days 7 and 14. On day 21 of culture, T cells were analyzed for their ability to secrete IFN-γ in response to stimulation with SOX2 peptides incorporated in the NPs. Blank NP–loaded DCs were used to stimulate T cells as negative controls. The figure is representative of experiments with three different healthy donors.

Combinatorial targeting of DCs by NPs and role of cytokines in DC crosstalk

Prior studies targeting NPs to DCs have focused on single DC type, and an optimal DC subset for vaccine targeting has not been defined (25). We hypothesized that simultaneously targeting multiple DC subsets may yield superior T cell responses. To this end, we compared NPs targeting either DC-$SIGN^+$ cells or $BDCA3^+$ cells alone or in combination. The combination of NPs targeting both DC-SIGN and BDCA3 led to significantly greater activation of Ag-specific T cells compared with targeting either subset of DCs alone (Fig. 5D, 5E). To extend the combinatorial targeting to a cancer Ag, PBMCs from cancer patients ($n = 4$, with a diagnosis of either melanoma or myeloma) were stimulated with blank NPs or SOX2-loaded NPs decorated with anti-BDCA3 and anti–DC-SIGN Abs. Combinatorial targeting with BDCA3 and DC-SIGN Ab–labeled SOX2NPs led to stimulation of SOX2-specific T cells in two of the four patients tested (Fig. 5F).

We hypothesized that the mechanism underlying this potentiation of immune stimulation may involve crosstalk between two subsets of DCs and mediated in part by cytokines. We examined secretion of IFN-α, -β, -γ, and -λ, IL-1α, IL-4, IL-5, IL-6, IL-8, IL-10, IL-3, IL-15, IL-23, IL-12p70, and TNF-α by NP-loaded DCs. Exposure of $BDCA3^+$ DCs to NPs leads to enhanced secretion of IFN-λ, IL-15, IL-6, IL-8, and TNF-α (Fig. 6A). Exposure to poly(I:C)-carrying particles did not further enhance these cytokine responses (data not shown). Exposure of Mo-DC–$SIGN^+$ DCs to NPs leads to enhanced secretion of IL-15, IL-6, IL-8, and TNF-α (Fig. 6A). Addition of LPS-decorated particles led to further increase in IL-6 (218 versus 614 pg/ml; $p = 0.0001$), TNF-α (164 versus 1003 pg/ml; $p = 0.017$), IL-13(10 versus 100 pg/ml; $p = 0.02$), and IL-23 (19 versus 64 pg/ml; $p = 0.02$) when compared with NPs alone. As the proportion of $BDCA3^+$ MDCs is much lower than other myeloid subsets, we reasoned that this subpopulation may be an important component of the crosstalk. We were particularly interested in examining the role of IL-15, IFN-λ, and IL-6 because these cytokines have been shown to be important for T cell activation. Ab-mediated blockade of IL-15 inhibited the potentiation of T cell activation seen with combinatorial DC targeting. In contrast, blockade of IFN-λ or IL-6 did not lead to significant inhibition of T cell activation (Fig. 6B). Together these data demonstrate that IL-15 signaling during combinatorial DC targeting plays an important role in the enhanced activation of T cell responses observed with combinatorial targeting of DC-$SIGN^+$ and $BDCA3^+$ DCs.

Discussion

In this study, we have shown that simultaneously targeting Ag-bearing NPs to multiple human DC subsets leads to superior immune activation. Therefore, these data suggest that the optimal strategy for targeting DCs may not lie in targeting a specific subset, as is currently being pursued (5), but rather concurrently targeting multiple DC subsets. The concept that optimal activation of immune responses may involve simultaneous activation of multiple DC subsets has also emerged from studies of protective immunity to pathogens (21, 33). It is notable that the yellow fever vaccine, which is one of the most potent vaccines in humans, does indeed target multiple DC subsets in vivo (34). Similarly, Kastenmuller et al. (35) demonstrated that protective immunity following a protein–TLR agonist conjugate vaccine required the engagement of multiple DC subsets. These data therefore have clear implica-

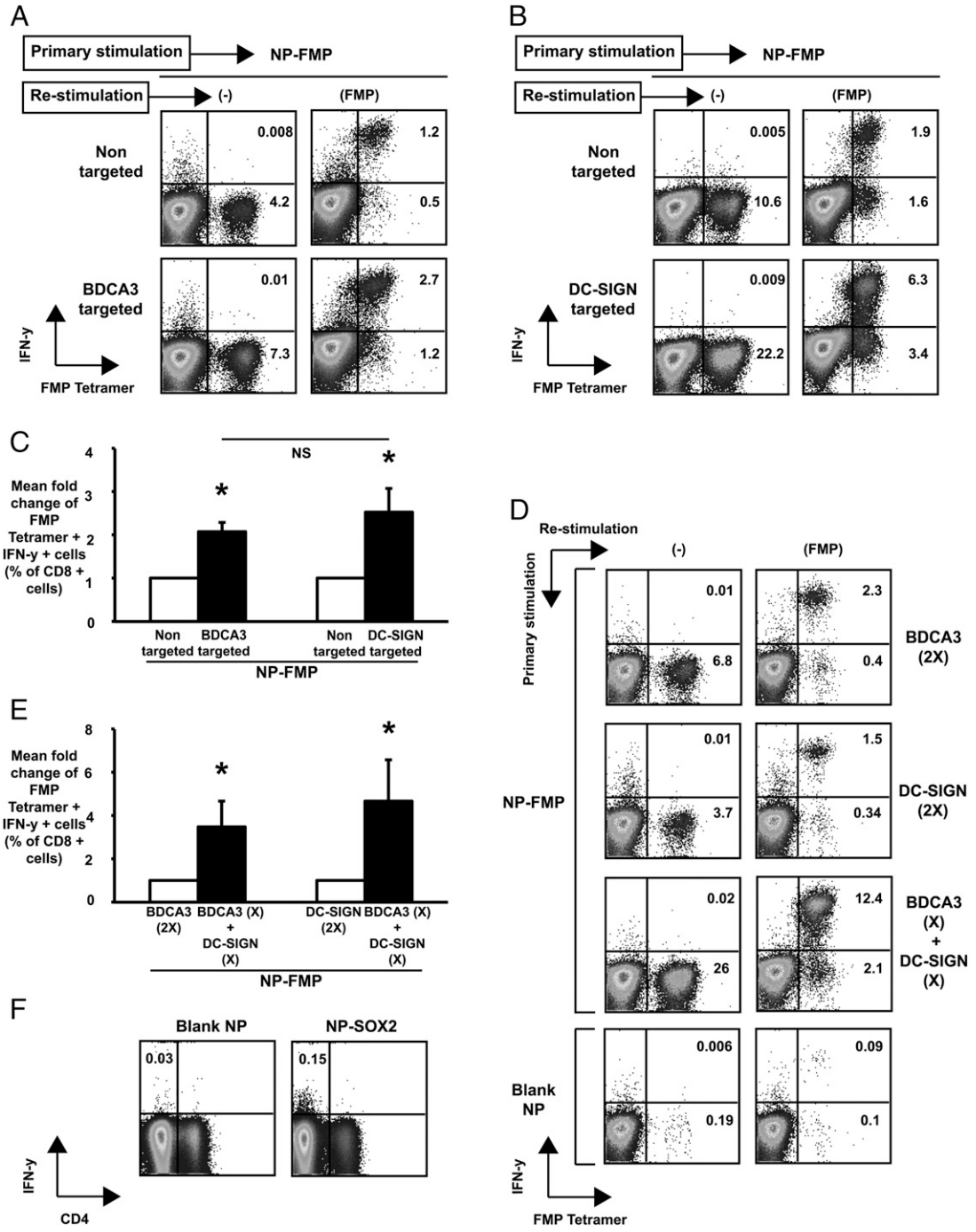

FIGURE 5. Combinatorial targeting of NPs to BDCA3$^+$ and DC-SIGN$^+$ DC subsets potentiates immune response. NP-FMP were conjugated with anti-BDCA3 or anti–DC-SIGN Abs through avidin–biotin interactions. They were then added to PBMCs to evaluate the effect of targeting. Nontargeted NP-FMP were used as negative controls. (**A**) PBMCs ($n = 3$) were pulsed with BDCA3-targeted or nontargeted NP-FMP (peptide concentration of 0.05 μg/ml). After 12–14 d of culture, they were restimulated with soluble FMP to evaluate IFN-γ production by FMP tetramer$^+$ CD8 T cells using flow cytometry. Figure shows a representative dot plot. (**B**) PBMCs ($n = 4$) were pulsed with DC-SIGN targeted or nontargeted NP-FMP (peptide concentration of 0.05 μg/ml). After 12–14 d of culture, they were restimulated with soluble FMP to evaluate IFN-γ production by FMP tetramer$^+$ CD8 T cells using flow cytometry. The figure shows a representative dot plot. (**C**) Figure shows induction of FMP-specific T cells using FMP-loaded NPs or FMP-loaded NPs decorated with either anti-BDCA3$^+$ ($n = 3$) or anti-DCSIGN Abs ($n = 4$). Bar graph shows mean fold change (compared with nontargeted NPs) of FMP tetramer$^+$ IFN-γ–secreting CD8 T cells generated under different stimulation conditions. *$p < 0.05$. (**D**) BDCA3-targeted NP-FMP (2× = peptide concentration of 0.05 μg/ml), DC-SIGN–targeted NP-FMP (2× = peptide concentration of 0.05 μg/ml), or a combination of the two (X+X = peptide concentrations of 0.025 μg/ml each) was added to PBMCs to study the effect of combinatorial targeting. BDCA3-targeted and DC-SIGN–targeted NP-FMP were conjugated with biotin-LPS and biotin-poly(I:C), respectively. Blank NPs (Blank NP) were used as negative controls. After 10–14 d, the cells were restimulated with soluble FMP (5 μg/ml) in the presence of anti-CD28 and anti-CD49d and analyzed for production of IFN-γ by FMP tetramer$^+$ T cells using flow cytometry. Figure shows dot plot from a representative experiment. Cells are gated on CD3$^+$ CD8$^+$ T cells. (**E**) Figure shows data from seven different healthy donors. Bars show mean fold increase in FMP tetramer$^+$ IFN-γ–secreting CD8+ T cells in cultures stimulated by combinatorial DC targeting with BDCA3- and DC-SIGN–conjugated NP-FMP, compared with those cultures stimulated with only BDCA3-targeted NP-FMP or DC-SIGN–targeted NP-FMP. *$p = 0.03$ for PBMCs stimulated with either BDCA3-targeted NP-FMP or DC-SIGN–targeted NP- FMP versus those stimulated with BDCA3-targeted (*Figure legend continues*)

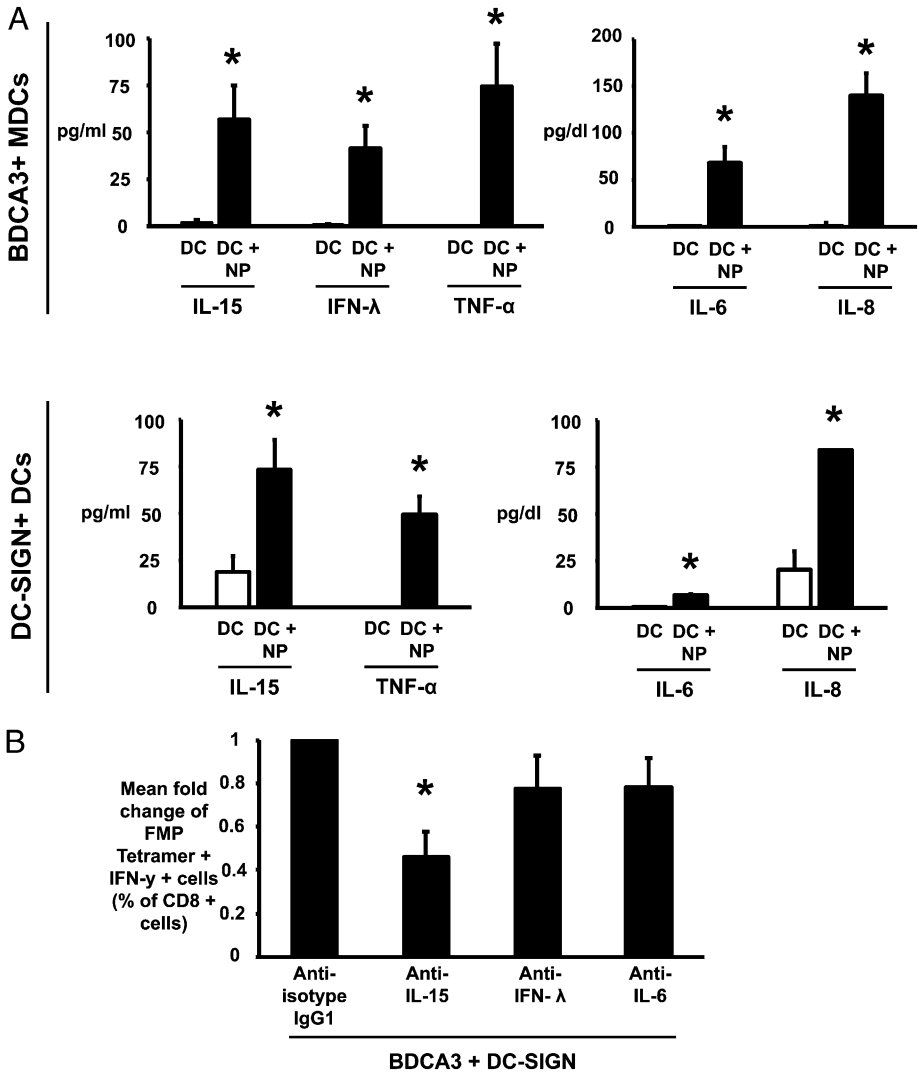

FIGURE 6. Combinatorial targeting to BDCA3$^+$ and DC-SIGN$^+$ DC subsets potentiates immune response through an IL-15–dependent mechanism. (**A**) The effects of NPs on isolated BDCA3$^+$ MDCs and DC-SIGN$^+$ Mo-DCs were studied by incubating the cells overnight with NP-FMP (peptide concentration 0.05 μg/ml) at 37°C. The supernatants were then collected and analyzed by VeriPlex Human Cytokine ELISA Kit. BDCA3$^+$ MDCs and DC-SIGN DCs incubated alone were used as negative controls. The graph shows mean cytokine expression levels (IL-15, IFN-λ, TNF-α, IL-6, and IL8) per 30,000 APCs ± SEM for cells obtained from three different healthy donors. *$p < 0.05$. (**B**) PBMCs were targeted with BDCA3- and DC-SIGN–coated NP-FMP in the presence of IL-15 blocking Ab, IFN-λ blocking Ab, IL-6 blocking Ab or isotype control Ab. After 10–12 d, the cultures were analyzed for the presence of FMP tetramer$^+$, IFN-γ–secreting CD8 T cells. Bar graph shows fold decrease in FMP tetramer$^+$ IFN-γ–producing CD8 T cells in cultures with blocking Abs compared with cultures with isotype control Ab ($n = 4$ different donors). *$p = 0.038$.

tions for the design of DC-targeting NP (or other) vaccines, as they suggest a need to consider simultaneous targeting of different DC subsets.

Integrative synergy with recruitment of diverse DC subsets may in principle be due to multiple mechanisms, including differences in their functional properties (2). Recent studies suggest that in contrast to murine DCs, most human DC subsets may be quite similar in terms of Ag cross-presentation and phagocytic function (23). Therefore, enhanced immune activation with combinatorial targeting may instead be due to crosstalk, such as that mediated by cytokines released by these DC subsets. BDCA3$^+$ MDCs (or their murine equivalent) are known to secrete IFN-λ as well as IL-15 upon activation (36–41). Our data suggest that IL-15–mediated signaling, but not IFN-λ released in the DC cultures, is important for the enhanced immune activation that we observed following combinatorial targeting involving BDCA3$^+$ MDCs. Trans-presentation of IL-15 by CD8α$^+$ DCs (murine equivalents of BDCA3$^+$ DCs) was shown to play a role in expansion of memory T cells (39, 42). IL-15 is already well known to activate MDCs and enhance their APC function (38, 43). Further studies are needed to better define the optimal combinations of DCs to target. One of the challenges in the studies of human DC subsets in vivo relates to differences in the biology of murine versus human DCs (23). It is not clear that this biology is faithfully reproduced yet in humanized mice in vivo (44), and therefore formal evaluation of DC crosstalk in humans in vivo may require careful human studies to improve vaccine design.

The novel NP platform described in this article has clear implications for translation to the clinic as the safety of PLGA NPs is already well established (8). The decoration of NPs with avidin as used in this study provides a simple yet effective strategy to generate NPs targeting different cell types using biotinylated Abs (27). In this study we have also shown that NPs can be easily encapsulated with complex peptide mixtures and

NP-FMP and DC SIGN–targeted NP-FMP. (**F**). Blank NP or SOX2 peptide–loaded DCs (5 μg/ml individual peptide) were coated with anti-BDCA3 or anti–DC-SIGN Ab, and a combination of BDCA3$^+$- and DC-SIGN$^+$–coated NPs (as in D) were used to stimulate PBMCs from cancer patients ($n = 4$) in the presence of IL-2, IL-7, and IL-15. At 15 d later, the cells were restimulated with soluble SOX2 peptide mix (5 μg/ml) in the presence of anti-CD28 and anti-CD49D and analyzed for production of IFN-γ using flow cytometry. Figure shows dot plot from a representative experiment where SOX2-reactive T cells could be stimulated. Cells are gated on CD3$^+$ T cells.

therefore effectively serve as poly-epitope vaccines. Generation of immunity against multiple epitopes may be particularly important in the context of immunity to pathogens and tumors. The demonstration that NPs loaded with overlapping peptide libraries (as shown in this article for SOX2) (45) can induce immunity provides a novel platform for clinical evaluation of NP-based vaccines irrespective of the HLA type. Furthermore, the ability to load multiple peptides also makes this technology readily amenable to personalized cancer vaccines, such as those against oncogenic mutation–derived peptides in tumor cells. Recent advances in engineering of these materials, including nanogels, can also be adapted toward combinatorial targeting of multiple DC subsets with poly-epitope vaccines against pathogens and tumors (46).

Disclosures

The authors have no financial conflicts of interest.

References

1. Steinman, R. M., and J. Banchereau. 2007. Taking dendritic cells into medicine. *Nature* 449: 419–426.
2. Palucka, K., and J. Banchereau. 2013. Human dendritic cell subsets in vaccination. *Curr. Opin. Immunol.* 25: 396–402.
3. Palucka, K., and J. Banchereau. 2013. Dendritic-cell-based therapeutic cancer vaccines. *Immunity* 39: 38–48.
4. Bandyopadhyay, A., R. L. Fine, S. Demento, L. K. Bockenstedt, and T. M. Fahmy. 2011. The impact of nanoparticle ligand density on dendritic-cell targeted vaccines. *Biomaterials* 32: 3094–3105.
5. Dhodapkar, M. V., M. Sznol, B. Zhao, D. Wang, R. D. Carvajal, M. L. Keohan, E. Chuang, R. E. Sanborn, J. Lutzky, J. Powderly, et al. 2014. Induction of antigen-specific immunity with a vaccine targeting NY-ESO-1 to the dendritic cell receptor DEC-205. *Sci. Transl. Med.* 6: 232ra51.
6. Paulis, L. E., S. Mandal, M. Kreutz, and C. G. Figdor. 2013. Dendritic cell-based nanovaccines for cancer immunotherapy. *Curr. Opin. Immunol.* 25: 389–395.
7. Cruz, L. J., P. J. Tacken, F. Rueda, J. C. Domingo, F. Albericio, and C. G. Figdor. 2012. Targeting nanoparticles to dendritic cells for immunotherapy. *Methods Enzymol.* 509: 143–163.
8. Metcalfe, S. M., and T. M. Fahmy. 2012. Targeted nanotherapy for induction of therapeutic immune responses. *Trends Mol. Med.* 18: 72–80.
9. Ali, O. A., D. Emerich, G. Dranoff, and D. J. Mooney. 2009. In situ regulation of DC subsets and T cells mediates tumor regression in mice. *Sci. Transl. Med.* 1: 8ra19.
10. Kasturi, S. P., I. Skountzou, R. A. Albrecht, D. Koutsonanos, T. Hua, H. I. Nakaya, R. Ravindran, S. Stewart, M. Alam, M. Kwissa, et al. 2011. Programming the magnitude and persistence of antibody responses with innate immunity. *Nature* 470: 543–547.
11. Demento, S. L., S. C. Eisenbarth, H. G. Foellmer, C. Platt, M. J. Caplan, W. Mark Saltzman, I. Mellman, M. Ledizet, E. Fikrig, R. A. Flavell, and T. M. Fahmy. 2009. Inflammasome-activating nanoparticles as modular systems for optimizing vaccine efficacy. *Vaccine* 27: 3013–3021.
12. Goldinger, S. M., R. Dummer, P. Baumgaertner, D. Mihic-Probst, K. Schwarz, A. Hammann-Haenni, J. Willers, C. Geldhof, J. O. Prior, T. M. Kündig, et al. 2012. Nano-particle vaccination combined with TLR-7 and -9 ligands triggers memory and effector CD8$^+$ T-cell responses in melanoma patients. *Eur. J. Immunol.* 42: 3049–3061.
13. Schreibelt, G., L. J. Klinkenberg, L. J. Cruz, P. J. Tacken, J. Tel, M. Kreutz, G. J. Adema, G. D. Brown, C. G. Figdor, and I. J. de Vries. 2012. The C-type lectin receptor CLEC9A mediates antigen uptake and (cross-)presentation by human blood BDCA3+ myeloid dendritic cells. *Blood* 119: 2284–2292.
14. Tacken, P. J., W. Ginter, L. Berod, L. J. Cruz, B. Joosten, T. Sparwasser, C. G. Figdor, and A. Cambi. 2011. Targeting DC-SIGN via its neck region leads to prolonged antigen residence in early endosomes, delayed lysosomal degradation, and cross-presentation. *Blood* 118: 4111–4119.
15. Tacken, P. J., I. S. Zeelenberg, L. J. Cruz, M. A. van Hout-Kuijer, G. van de Glind, R. G. Fokkink, A. J. Lambeck, and C. G. Figdor. 2011. Targeted delivery of TLR ligands to human and mouse dendritic cells strongly enhances adjuvanticity. *Blood* 118: 6836–6844.
16. Cruz, L. J., P. J. Tacken, R. Fokkink, B. Joosten, M. C. Stuart, F. Albericio, R. Torensma, and C. G. Figdor. 2010. Targeted PLGA nano- but not microparticles specifically deliver antigen to human dendritic cells via DC-SIGN in vitro. *J. Control. Release* 144: 118–126.
17. Tel, J., S. P. Sittig, R. A. Blom, L. J. Cruz, G. Schreibelt, C. G. Figdor, and I. J. de Vries. 2013. Targeting uptake receptors on human plasmacytoid dendritic cells triggers antigen cross-presentation and robust type I IFN secretion. *J. Immunol.* 191: 5005–5012.
18. Cruz, L. J., P. J. Tacken, J. M. Pots, R. Torensma, S. I. Buschow, and C. G. Figdor. 2012. Comparison of antibodies and carbohydrates to target vaccines to human dendritic cells via DC-SIGN. *Biomaterials* 33: 4229–4239.
19. Demento, S. L., A. L. Siefert, A. Bandyopadhyay, F. A. Sharp, and T. M. Fahmy. 2011. Pathogen-associated molecular patterns on biomaterials: a paradigm for engineering new vaccines. *Trends Biotechnol.* 29: 294–306.
20. Dudziak, D., A. O. Kamphorst, G. F. Heidkamp, V. R. Buchholz, C. Trumpfheller, S. Yamazaki, C. Cheong, K. Liu, H. W. Lee, C. G. Park, et al. 2007. Differential antigen processing by dendritic cell subsets in vivo. *Science* 315: 107–111.
21. Pulendran, B., H. Tang, and T. L. Denning. 2008. Division of labor, plasticity, and crosstalk between dendritic cell subsets. *Curr. Opin. Immunol.* 20: 61–67.
22. Luci, C., and F. Anjuère. 2011. IFN-λs and BDCA3+/CD8α+ dendritic cells: towards the design of novel vaccine adjuvants? *Expert Rev. Vaccines* 10: 159–161.
23. Segura, E., M. Durand, and S. Amigorena. 2013. Similar antigen cross-presentation capacity and phagocytic functions in all freshly isolated human lymphoid organ-resident dendritic cells. *J. Exp. Med.* 210: 1035–1047.
24. Cohn, L., B. Chatterjee, F. Esselborn, A. Smed-Sörensen, N. Nakamura, C. Chalouni, B. C. Lee, R. Vandlen, T. Keler, P. Lauer, et al. 2013. Antigen delivery to early endosomes eliminates the superiority of human blood BDCA3+ dendritic cells at cross presentation. *J. Exp. Med.* 210: 1049–1063.
25. Kreutz, M., P. J. Tacken, and C. G. Figdor. 2013. Targeting dendritic cells—why bother? *Blood* 121: 2836–2844.
26. Fahmy, T. M., S. L. Demento, M. J. Caplan, I. Mellman, and W. M. Saltzman. 2008. Design opportunities for actively targeted nanoparticle vaccines. *Nanomedicine (Lond)* 3: 343–355.
27. Park, J., T. Mattessich, S. M. Jay, A. Agawu, W. M. Saltzman, and T. M. Fahmy. 2011. Enhancement of surface ligand display on PLGA nanoparticles with amphiphilic ligand conjugates. *J. Control. Release:* 156: 109–115.
28. Fahmy, T. M., R. M. Samstein, C. C. Harness, and W. Mark Saltzman. 2005. Surface modification of biodegradable polyesters with fatty acid conjugates for improved drug targeting. *Biomaterials* 26: 5727–5736.
29. Dhodapkar, K. M., J. L. Kaufman, M. Ehlers, D. K. Banerjee, E. Bonvini, S. Koenig, R. M. Steinman, J. V. Ravetch, and M. V. Dhodapkar. 2005. Selective blockade of inhibitory Fcgamma receptor enables human dendritic cell maturation with IL-12p70 production and immunity to antibody-coated tumor cells. *Proc. Natl. Acad. Sci. USA* 102: 2910–2915.
30. Bass, A. J., H. Watanabe, C. H. Mermel, S. Yu, S. Perner, R. G. Verhaak, S. Y. Kim, L. Wardwell, P. Tamayo, I. Gat-Viks, et al. 2009. SOX2 is an amplified lineage-survival oncogene in lung and esophageal squamous cell carcinomas. *Nat. Genet.* 41: 1238–1242.
31. Dhodapkar, K. M., S. N. Gettinger, R. Das, H. Zebroski, and M. V. Dhodapkar. 2013. SOX2-specific adaptive immunity and response to immunotherapy in non-small cell lung cancer. *OncoImmunology* 2: e25205.
32. Spisek, R., A. Kukreja, L. C. Chen, P. Matthews, A. Mazumder, D. Vesole, S. Jagannath, H. A. Zebroski, A. J. Simpson, G. Ritter, et al. 2007. Frequent and specific immunity to the embryonal stem cell-associated antigen SOX2 in patients with monoclonal gammopathy. *J. Exp. Med.* 204: 831–840.
33. Pulendran, B., J. Z. Oh, H. I. Nakaya, R. Ravindran, and D. A. Kazmin. 2013. Immunity to viruses: learning from successful human vaccines. *Immunol. Rev.* 255: 243–255.
34. Querec, T., S. Bennouna, S. Alkan, Y. Laouar, K. Gorden, R. Flavell, S. Akira, R. Ahmed, and B. Pulendran. 2006. Yellow fever vaccine YF-17D activates multiple dendritic cell subsets via TLR2, 7, 8, and 9 to stimulate polyvalent immunity. *J. Exp. Med.* 203: 413–424.
35. Kastenmüller, K., U. Wille-Reece, R. W. Lindsay, L. R. Trager, P. A. Darrah, B. J. Flynn, M. R. Becker, M. C. Udey, B. E. Clausen, B. Z. Igyarto, et al. 2011. Protective T cell immunity in mice following protein-TLR7/8 agonist-conjugate immunization requires aggregation, type I IFN, and multiple DC subsets. *J. Clin. Invest.* 121: 1782–1796.
36. Lauterbach, H., B. Bathke, S. Gilles, C. Traidl-Hoffmann, C. A. Luber, G. Fejer, M. A. Freudenberg, G. M. Davey, D. Vremec, A. Kallies, et al. 2010. Mouse CD8alpha+ DCs and human BDCA3+ DCs are major producers of IFN-lambda in response to poly IC. *J. Exp. Med.* 207: 2703–2717.
37. Poulin, L. F., M. Salio, E. Griessinger, F. Anjos-Afonso, L. Craciun, J. L. Chen, A. M. Keller, O. Joffre, S. Zelenay, E. Nye, et al. 2010. Characterization of human DNGR-1+ BDCA3+ leukocytes as putative equivalents of mouse CD8alpha+ dendritic cells. *J. Exp. Med.* 207: 1261–1271.
38. Dubsky, P., H. Saito, M. Leogier, C. Dantin, J. E. Connolly, J. Banchereau, and A. K. Palucka. 2007. IL-15-induced human DC efficiently prime melanoma-specific naive CD8+ T cells to differentiate into CTL. *Eur. J. Immunol.* 37: 1678–1690.
39. Sosinowski, T., J. T. White, E. W. Cross, C. Haluszczak, P. Marrack, L. Gapin, and R. M. Kedl. 2013. CD8α+ dendritic cell trans presentation of IL-15 to naive CD8+ T cells produces antigen-inexperienced T cells in the periphery with memory phenotype and function. *J. Immunol.* 190: 1936–1947.
40. Anguille, S., E. Lion, J. Tel, I. J. de Vries, K. Couderé, P. D. Fromm, V. F. Van Tendeloo, E. L. Smits, and Z. N. Berneman. 2012. Interleukin-15-induced CD56(+) myeloid dendritic cells combine potent tumor antigen presentation with direct tumoricidal potential. *PLoS ONE* 7: e51851.
41. Colpitts, S. L., T. A. Stoklasek, C. R. Plumlee, J. J. Obar, C. Guo, and L. Lefrançois. 2012. Cutting edge: the role of IFN-α receptor and MyD88 signaling in induction of IL-15 expression in vivo. *J. Immunol.* 188: 2483–2487.
42. Stonier, S. W., and K. S. Schluns. 2010. Trans-presentation: a novel mechanism regulating IL-15 delivery and responses. *Immunol. Lett.* 127: 85–92.

43. Perera, P. Y., J. H. Lichy, T. A. Waldmann, and L. P. Perera. 2012. The role of interleukin-15 in inflammation and immune responses to infection: implications for its therapeutic use. *Microbes Infect.* 14: 247–261.
44. Akkina, R. 2013. Human immune responses and potential for vaccine assessment in humanized mice. *Curr. Opin. Immunol.* 25: 403–409.
45. Dhodapkar, M. V., and K. M. Dhodapkar. 2011. Vaccines targeting cancer stem cells: are they within reach? *Cancer J.* 17: 397–402.
46. Look, M., E. Stern, Q. A. Wang, L. D. DiPlacido, M. Kashgarian, J. Craft, and T. M. Fahmy. 2013. Nanogel-based delivery of mycophenolic acid ameliorates systemic lupus erythematosus in mice. *J. Clin. Invest.* 123: 1741–1749.

SUPPLEMENTAL DATA:

Supplemental Table 1: Composition of nanoparticles

Nanoparticles	**No. of individual peptide components**	**Amount of individual peptide/NP** (ug of individual peptide /mg of NP)
NP-FMP	1	9
NP-CEF	32	0.5625
NP-SOX2	22	4.1616

Supplemental Table 2: Description of individual peptide components of SOX2 pool peptide, encapsulated in NP-SOX2

Serial Number	SOX2 Peptide Sequence
1	LGAEWKLLSETEKR
2	EWKLLSETEKRPFI
3	LLSETEKRPFIDEAK
4	TEKRPFIDEAKRLRA
5	PFIDEAKRLRALHMK
6	EAKRLRALHMKEH
7	KRLRALHMKEHPDYK
8	ALHMKEHPDYKYRPR
9	KEHPDYKYRPRRKTK
10	DYKYRPRRKTKTLMK
11	RPRRKTKTLMKKDKY
12	KTKTLMKKDKYTLPG
13	LMKKDKYTLPGGLLA
14	DKYTLPGGLLAPGG
15	TLPGGLLAPGGNSMA
16	GLLAPGGNSMASGVG
17	PGGNSMASGVGVGAG
18	SMASGVGVGAGLGAG
19	GVGVGAGLGAGVNQR
20	GAGLGAGVNQRMDSY
21	GAGVNQRMDSYAHM
22	VNQRMDSYAHMNGWS

Supplemental Table 3: Description of individual peptide components of CEF pool peptide used for re-stimulation of cells primed with NP-CEF (shown in Fig.3d)

Peptide	HLA Allele	Virus	Protein & Region	Peptide Sequence
Pep 1	A1	INFLUENZA A	PB1 (591 – 599)	VSDGGPNLY
Pep 2	A2	EBV	BMLF1 (259 – 267)	GLCTLVAML
Pep 3	A2	INFLUENZA A	MATRIX 1 (58 – 66)	GILGFVFTL
Pep 4	A3	INFLUENZA A	NP (265 – 273)	ILRGSVAHK
Pep 5	A3	EBV	BRLF1 (148 -156)	RVRAYTYSK
Pep 6	A3	EBV	EBNA 3A (603 – 611)	RLRAEAQVK
Pep 7	A11	EBV	EBNA 3B (416 – 424)	IVTDFSVIK
Pep 8	A11	EBV	BRLF1 (134 – 143)	ATIGTAMYK
Pep 9	A24	EBV	BRLF1 (28 – 37)	DYCNVLNKEF
Pep 10	A68	INFLUENZA A	NP (91 – 99)	KTGGPIYKR
Pep 11	B7	EBV	EBNA 3A (379-387)	RPPIFIRRL
Pep 12	B8	EBV	EBNA 3A (158 – 166)	QAKWRLQTL
Pep 13	B8	EBV	EBNA 3A (325-333)	FLRGRAYGL
Pep 14	B8	EBV	BZLF1 (190 – 197)	RAKFKQLL
Pep 15	B27	EBV	EBNA 3C (258 – 266)	RRIYDLIEL
Pep 16	B27	INFLUENZA A	NP (383 – 391)	SRYWAIRTR
Pep 17	B35	EBV	EBNA 3A (458 – 466)	YPLHEQHGM
Pep 18	B44	HCMV	Pp65 (512 – 521)	EFFWDANDIY

*EBV = Epstein Barr virus, HCMV = Human cytomegalovirus.

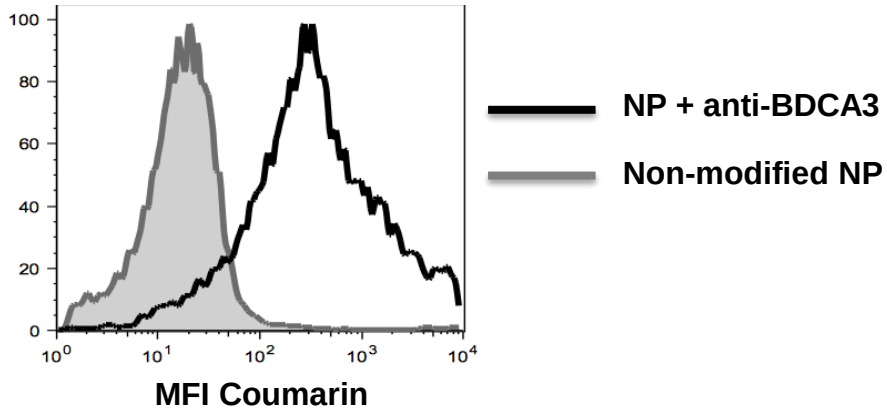

Supplemental Fig. 1a: Evaluation of coupling of biotinylated antibody on the surface of avidin-coated NP. To detect the presence of biotin-labeled BDCA3 antibody (mouse IgG1, clone AD5-14H12) on the surface, NP were stained with rat anti-mouse IgG1-APC (clone X56) for 15 minutes and analyzed by FACSCalibur.

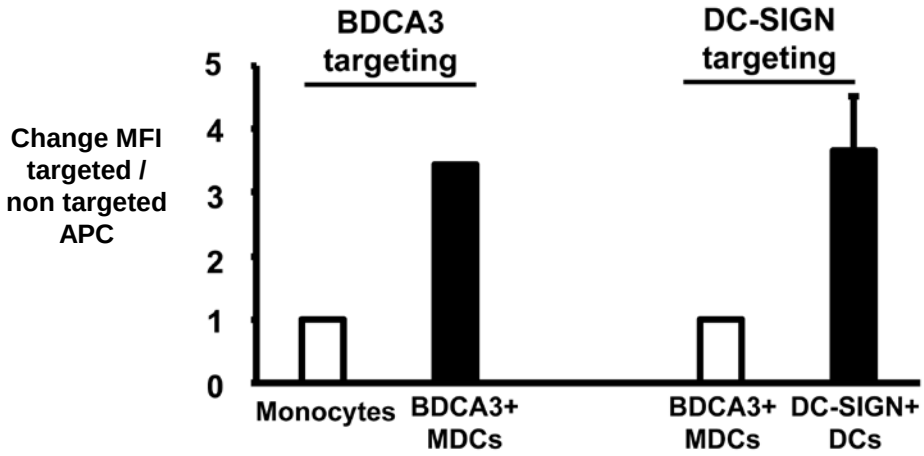

Supplemental Fig. 1b: Coumarin-labeled NPs were coated with either anti-BDCA3 or anti DC-SIGN antibody and co-cultured with PBMCs for 30 min at 4^0C. Figure shows change MFI of coumarin in targeted APCs versus non-targeted APCs.

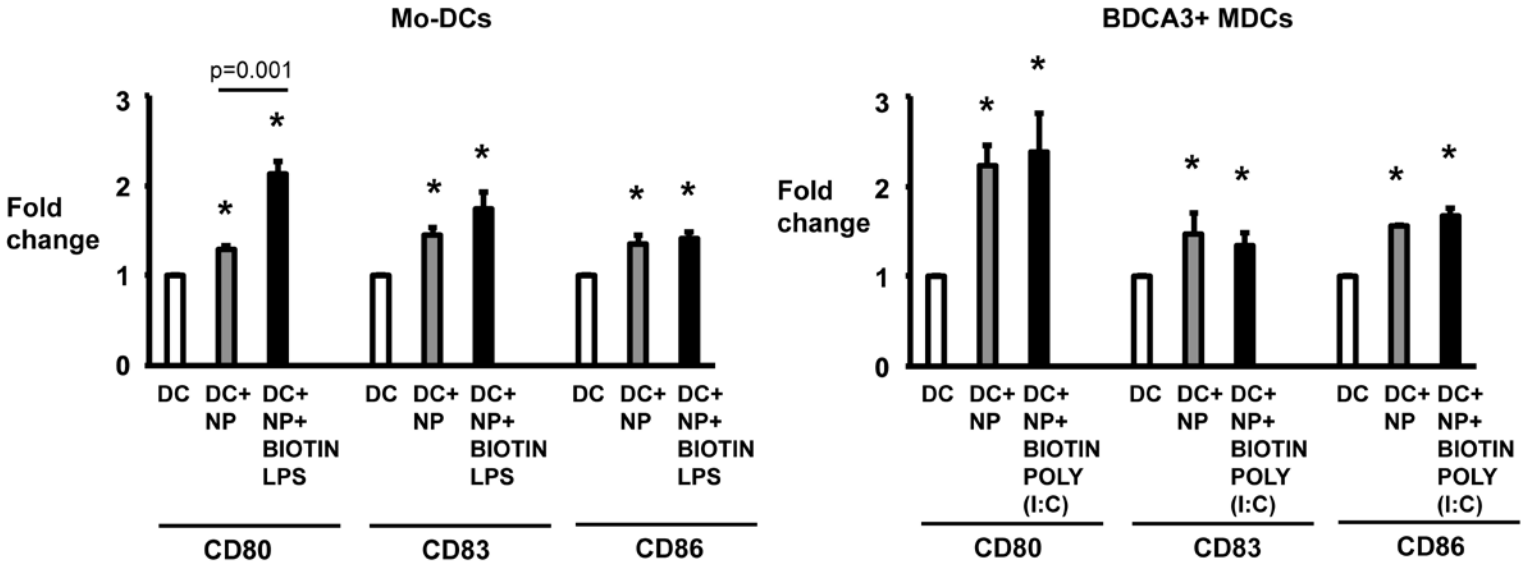

Supplemental Fig. 1c: Bar graphs shows fold change MFI of CD80, CD83 and CD86 in DCs cultured alone or with NPs or NPs coated with TLRs (LPS or Poly (I:C). * represents significant p value compared to DC alone (DC).